Simple Model for the Deformation-Induced Relaxation of Glassy Polymers

S. M. Fielding,[1] R. G. Larson,[2] and M. E. Cates[3]

[1]Department of Physics, Durham University, Science Laboratories, South Road, Durham DH1 3LE, United Kingdom
[2]Department of Chemical Engineering, University of Michigan, Ann Arbor, Michigan 48109-2136, USA
[3]SUPA, School of Physics and Astronomy, The University of Edinburgh, JCMB Kings Buildings, Edinburgh, EH9 3JZ, United Kingdom

(Received 18 October 2011; published 25 January 2012)

Glassy polymers show ''strain hardening'': at constant extensional load, their flow first accelerates, then arrests. Recent experiments have found this to be accompanied by a striking and unexplained dip in the segmental relaxation time. Here we explain such behavior by combining a minimal model of flow-induced liquefaction of a glass with a description of the stress carried by strained polymers, creating a nonfactorable interplay between aging and strain-induced rejuvenation. Under constant load, liquefaction of segmental motion permits strong flow that creates polymer-borne stress. This slows the deformation enough for the segmental modes to revitrify, causing strain hardening.

DOI: 10.1103/PhysRevLett.108.048301 PACS numbers: 83.80.Va, 62.20.−x, 64.70.pj

Understanding the flow of polymeric materials is central to their manufacture and performance. After decades of progress, the flow properties of molten polymers are elegantly described by modern entanglement theories [1,2]. In use, however, most polymeric materials are not molten, but rigid. This conversion is commonly achieved by cooling to below the glass transition temperature T_g. In contrast to the molten case, satisfactory theories of polymer glass rheology remain elusive.

Just below T_g, polymer glasses undergo slow plastic deformation if stress is applied [3,4]. Similar plasticity is shown also by molecular, metallic, and colloidal glasses [5–7]. Our understanding of flow in such nonpolymeric glasses has improved greatly due to recent advances in microscopic [8,9] and mesoscopic [10–12] theory. Crucial to glass rheology is physical aging: a quiescent glass becomes more sluggish with time, rejuvenating under flow. This is captured schematically in minimal ''fluidity'' models, with a time evolution equation for a single structural relaxation rate (the fluidity) [13,14]. In the so-called ''simple-aging'' scenario, the structural relaxation time τ (or inverse fluidity) of the system at rest increases linearly with its age [4,10,15]. A slow steady flow cuts off this growth at the inverse flow rate.

In polymeric glasses, new properties emerge from the interplay between polymeric and glassy degrees of freedom. Particularly striking is the evolution of the segmental relaxation time $\tau(t)$, controlling the rate of local rearrangements, when a load is applied. Recently, Lee *et al.* [3,16] showed that $\tau(t)$ falls steadily during the early stages of elongational deformation, and then more sharply, reaching a small fraction $\sim 10^{-3.3}$ of its initial level before dramatically rising again, as the local strain rate starts to drop on entering the ''strain hardening'' regime. While elements of this scenario have been confirmed in coarse-grained and molecular simulations [17–20], no convincing theoretical picture has yet emerged.

In [3], the results for $\tau(t)$ were found inconsistent with the theory of Eyring [21] and with a more recent model [11] (see also [22–24]) involving similar precepts. The Eyring-like assumption of a purely stress-dependent fluidity, introduced for polymers in [25], is fundamentally at odds with aging in glasses, whose fluidity is time dependent at constant stress [4,10,15]. Previous work to incorporate aging and flow rejuvenation into polymer glass theory has led to the Eindhoven glassy polymer (EGP) model [26], where viscosity is controlled by a state parameter S that is age and strain dependent. However, in the EGP model aging and rejuvenation have factorable effects on S: strain-induced rejuvenation causes cumulative losses of structure (reductions in S) which multiplicatively reduces all subsequent relaxation times. This is not what theories of simple glasses predict [10,13,14]. The EGP's precepts may thus be unsuited to the regime of strong fluidization, as addressed experimentally in [3] and in recent glass rheology theories [8–10,13,14].

Despite recent efforts [11,22,24,27–29], creating a complete theory of rheological aging in polymer glasses remains a formidable task. Here we show that a minimal model, combining just two key elements of any such theory (nonfactorable aging or rejuvenation, and the strain dependence of polymer-borne stresses), semiquantitatively explains many of the results reported in [3].

Our model describes polymeric dumbbells [2] suspended in a glassy ''solvent,'' whose microscopic relaxation time obeys a fluidity-type equation showing simple aging and flow rejuvenation. Despite our nomenclature, we do not require any actual solvent to be present: the separation between polymer and ''solvent'' instead divides the slow degrees of freedom of large sections of chain from the shorter-scale and faster relaxing modes that control local segmental dynamics. Our model thus follows lines developed in [25,26] but crucially differs in its treatment of aging and rejuvenation. For simplicity we treat the

dumbbells initially as purely elastic elements—as is valid in the molten state, where the elasticity is of entropic origin [2]. However, we later return to discuss the true nature of the polymer stress in polymeric glasses which is not solely entropic in character [24,28]. This might seemingly call into question our time-scale separation into "polymeric" and "solvent" degrees of freedom; however, recent careful experiments [30] and modeling [29] give clear evidence for such a separation.

Our model first defines a deviatoric stress tensor $\mathbf{\Sigma} = G^p(\boldsymbol{\sigma}^p - \mathbf{I}) + G^s(\boldsymbol{\sigma}^s - \mathbf{I})$ where $\boldsymbol{\sigma}^p$ and $\boldsymbol{\sigma}^s$ are dimensionless conformation tensors for polymer and "solvent," $G^{p,s}$ associated elastic moduli (see below), and $\mathbf{I}$ the unit tensor. We then adopt the following equations for the conformation tensors and solvent relaxation time τ:

$$\dot{\boldsymbol{\sigma}}^p + \mathbf{v}\cdot\boldsymbol{\nabla}\boldsymbol{\sigma}^p = \boldsymbol{\sigma}^p\cdot\boldsymbol{\nabla}\mathbf{v} + (\boldsymbol{\nabla}\mathbf{v})^T\cdot\boldsymbol{\sigma}^p - \alpha(\boldsymbol{\sigma}^p - \mathbf{I})/\tau, \tag{1}$$

$$\dot{\boldsymbol{\sigma}}^s + \mathbf{v}\cdot\boldsymbol{\nabla}\boldsymbol{\sigma}^s = \boldsymbol{\sigma}^s\cdot\boldsymbol{\nabla}\mathbf{v} + (\boldsymbol{\nabla}\mathbf{v})^T\cdot\boldsymbol{\sigma}^s - (\boldsymbol{\sigma}^s - \mathbf{I})/\tau, \tag{2}$$

$$\dot{\tau} + \mathbf{v}\cdot\boldsymbol{\nabla}\tau = 1 - (\tau - \tau_0)\lambda, \tag{3}$$

$$\lambda(\mathbf{D}) \equiv \mu\sqrt{2\mathrm{Tr}(\mathbf{D}.\mathbf{D})}. \tag{4}$$

Here $\mathbf{v}$ is the fluid velocity and $\mathbf{D} = [\boldsymbol{\nabla}\mathbf{v} + (\boldsymbol{\nabla}\mathbf{v})^T]/2$.

Equation (1) is the so-called "upper-convected Maxwell model" or UCM. In simple shear at rate $\dot{\gamma}$, its shear stress $G^p\sigma^p$ is governed by $\dot{\sigma}^p = \dot{\gamma} - \alpha\sigma^p/\tau$, reducing to the familiar (linear) Maxwell model. The UCM is the simplest extension of this to general flows that respects rotational and other invariances [2]. Physically, the UCM describes the dynamics of dumbbells; these carry a stress $G^p\boldsymbol{\sigma}^p$ and have a structural relaxation time $\tau^p = \tau/\alpha$, proportional to, but much larger than, that of the "solvent," τ. In the simplest models of dense, molten, but unentangled polymers, $\alpha = N^{-2}$ with N the polymerization index [2], whereas in a lightly crosslinked elastomeric network [3] one expects $\alpha = 0$. Consistent with its glassy nature, the solvent itself is viewed as a viscoelastic fluid. Bearing in mind that it represents shorter-scale polymeric degrees of freedom, we model this fluid using another UCM (2). Because there are more local than chain-scale degrees of freedom, we expect $G^s > G^p$.

Finally, the solvent's structural relaxation time τ obeys a fluidity-type equation (3), with the following two features. First, without flow, τ increases linearly in time at a (dimensionless) solidification rate $\dot{\tau}(\mathbf{D} = \mathbf{0})$ which for simplicity we set to unity. This embodies the simple aging scenario that emerges from mesoscopic models [10], whereby local configurations evolve into ever deeper traps. Second, with flow present, τ would, in the absence of such aging, itself undergo deformation-induced relaxation towards τ_0 which is a "fully rejuvenated" value. This relaxation occurs at a rate λ, proportional to a scalar measure of flow rate (with μ another dimensionless coefficient [2,9]). In steady shear ($\lambda = \mu\dot{\gamma}$), τ then varies inversely with strain rate $\dot{\gamma}$ in accord with microscopic theory [8]. For uniaxial elongation at strain rate $\dot{\varepsilon}$, (4) reduces to $\lambda = \mu\sqrt{3}|\dot{\varepsilon}|$. Note that in this simple fluidity model, the rejuvenation of τ is essentially strain induced [9] but, in contrast to the factorable model of [26], can be rapidly reversed by subsequent aging.

Our model is completed by the standard equations of mass and force balance for an incompressible fluid of negligible inertia: $\boldsymbol{\nabla}\cdot\mathbf{v} = 0$, and $\boldsymbol{\nabla}\cdot[\mathbf{\Sigma} + 2\eta\mathbf{D}] = 0$. (We add a small Newtonian viscosity η for purely numerical reasons [31].) We have solved our model numerically for uniaxial extension flows within a lubrication approximation appropriate to long cylindrical samples. Our numerical solutions address two cases [31]. One is an effectively infinite cylinder whose cross section remains spatially uniform, but is time dependent. The second is a finite cylinder perturbed to trigger an inherent "necking" instability (seen, in mild form, in [3]). We show next, however, that a semiquantitative account of the $\tau(t)$ response under elongational load is already predicted by applying our simple model to the infinite uniform cylinder.

In confronting the experimental data for $\tau(t)$ we first set α negligibly small, appropriate for a crosslinked material [3]. The experimental protocol of [3] determines the applied tensile force F; the initial relaxation time (t_w in our model) before applying the load; and the time t_u at which unload later occurs. There remain four material parameters in the model: G^p, G^s, τ_0, and μ. As detailed in [31], three of these are strongly constrained by measurements that do not involve the dip in the $\tau(t)$ curve. Indeed, G^p/F can be deduced from the asymptotic deformation in the strain-hardened regime just before unload; once G^p is known (we find $G^p = 6$ MPa) G^s and μ are in turn estimated from the step-change in τ during initial loading, and from the separately measured slope [3] of the "effective flow curve" $\dot{\varepsilon}(\tau)$. Hence, the only unconstrained parameter in fitting the dip in $\tau(t)$ is τ_0.

We find a good semiquantitative account of the strain curve and $\tau(t)$ data, up to but not beyond the point of unload, by choosing $\tau_0 \simeq 6$ s. (Unloading is addressed separately below.) Figure 1 shows not only the local strain and the segmental relaxation time $\tau(t)$, but also the tensile stresses $T^{p,s}$ carried by polymer and solvent, respectively. Key features of the experimental data, reproduced by our minimal model, include: (i) the initial drop in τ on applying the load; (ii) its subsequent further decline to a state of strong fluidization, with a sharp minimum $\tau_{\min}$ near the point of maximum elongation rate; and (iii) its rapid but decelerating rise from the minimum. Not only the initial tenfold drop in τ on loading but also the subsequent further sharp dip is quantitatively accounted for. Figure 2 shows τ as a function of the elongational stress, with breakdown of

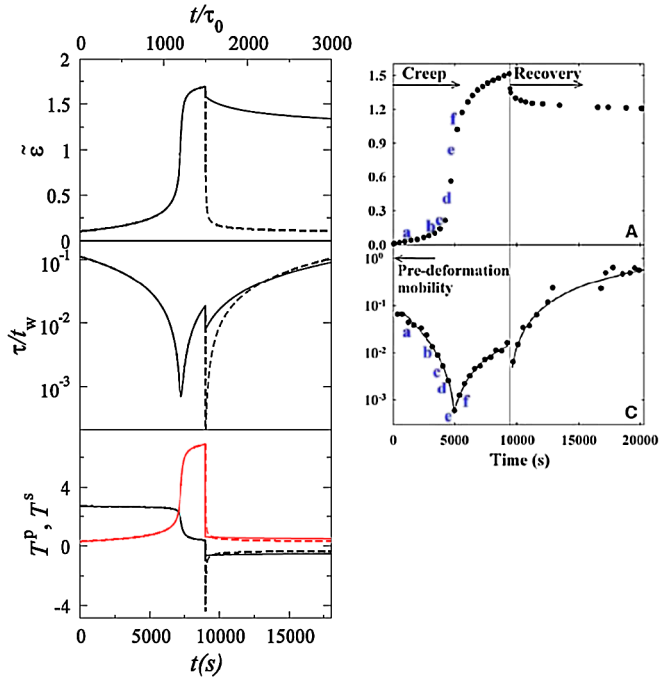

FIG. 1 (color online). Left Panels, solid curves: local strain $\tilde{\varepsilon} = \exp\varepsilon - 1$ [3], reduced relaxation time $\tau(t)/t_w$ and tensile stresses $T^{p,s} = G^{p,s}(\sigma_{zz}^{p,s} - \sigma_{xx}^{p,s})$ of the polymer (p) and solvent (s) during loading of an infinite uniform cylinder. Parameters $G^s/G^p = 8.5$, $\mu = 12.5$, $t_w/\tau_0 = 10^4$, $\tau_0 = 6$ s; applied force/initial area $f = 2.7G_p$. (The curve for T^p, in red online, initially lies below T^s but crosses it during strain hardening.) The unload results for the basic model ($\theta = 1$) is shown dashed; the solid curve after unload has $\theta = 0.1$. The horizontal axis is marked both in dimensionless model units (top) and real time (converted using τ_0), bottom. Right panels: Comparable experimental data for local strain and reduced relaxation time. (From [3]; reprinted by permission of AAAS.)

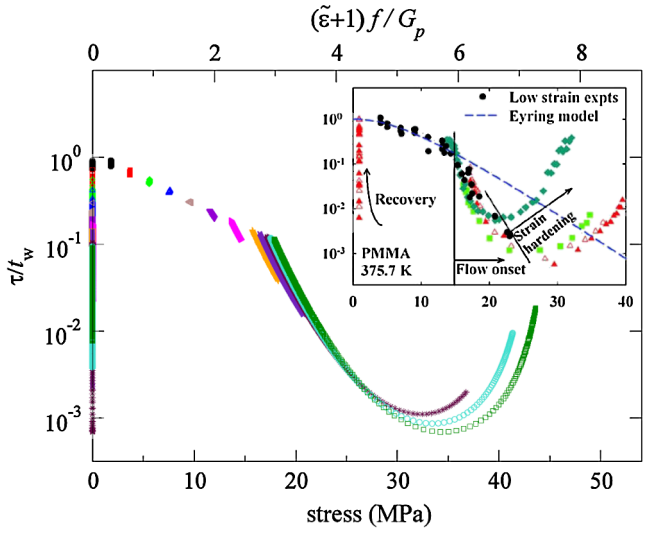

FIG. 2 (color online). Reduced relaxation time τ/t_w against actual stress in the infinite uniform cylinder. Parameter values $G^s/G^p = 8.5$, $\mu = 12.5$, $t_w/\tau_0 = 10^4$, $\tau_0 = 6$ s for a scaled applied force per initial area $F/G^p = 0.3$, 0.6, 0.9, 1.2, 1.5, 1.8, 2.1, 2.4, 2.5, 2.6, 2.65, 2.7 (increasing left to right). The unload time obeys $T_{\text{unload}} = 1500\tau_0$. The horizontal axis is marked both in dimensionless model units (top) and laboratory stress (bottom, as used in the inset; converted factor $G^p = 6$ MPa). These curves show qualitative agreement with the experimental data (from [3]; reprinted by permission of AAAS) (inset).

the Eyring-like expectation of a monotonic, single-valued plot. Figure 3 shows (on log-log) $\dot{\varepsilon}$ against $1/\tau$; this plot was found to collapse the experimental data in [3] and a similar, if lesser, effect is seen here. Considering the crudeness of our model (which represents polymers and solvent by a single mode each), this is remarkable agreement.

If our model is correct, the physics of all these effects is remarkably simple. The (preaged) "solvent" glass has a yield stress Σ_Y^s [in our model this obeys $\Sigma_Y^s = G^s g(\sqrt{3}\mu)$ with $g(y) \equiv 3y/(y-2)(y+1)$] which is initially exceeded by the applied load. After an initial step-down in τ caused by step strain on loading, the material yields and progressively fluidizes further; accordingly its strain rate accelerates, giving positive feedback and a collapse in τ. As deformation builds up, however, an ever growing share of the applied stress is instead carried by the stretching polymer chains. This causes the flow rate to drop, so that the solvent, whose stress now obeys $\Sigma^s < \Sigma_Y^s$, starts to solidify. This simple view of strain hardening also directly explains the remarkable behavior of $\tau(t)$.

Models that factorize aging and rejuvenation effects [26] are seriously challenged by the rapid recovery of τ after the dip. (A multimode spectrum [32] is unlikely to help here.) With simple aging, such factorization predicts $\tau \sim (t + t_w)f(\epsilon)$, so that if the segmental relaxation times falls from its predeformation value t_w to a small value $\tau = ft_w = \tau_{\min}$ at the dip, a tenfold recovery to $\tau \sim 10\tau_{\min}$ does not occur until $t \sim 10t_w \sim 6 \times 10^5$ s. This prediction is 100 times too long [3].

We have also performed numerical calculations in the case of a finite cylinder subject to a necking instability. More details, and an additional figure, are provided in [31]. Although our model is not predictive of sample shapes (which depend on the details of the perturbation used to initiate the neck), plots of $\tau(t)$, and sample radius $\rho(t)$, at three different initial positions along the sample are in qualitative accord with the experiments of [3]. The explanation given above for the temporal behavior of $\tau(t)$ during elongation of an infinite uniform cylinder remains equally valid for a finite, necked one.

To check that our model also behaves reasonably in strain-controlled flows, we have calculated stress responses for startup of steady elongation or compression. These show an overshoot (see [31]) whose height varies as $\ln(\dot{\varepsilon}t_w)$, as seen in simple aging fluids [10], and in broad accord with the polymer glass literature.

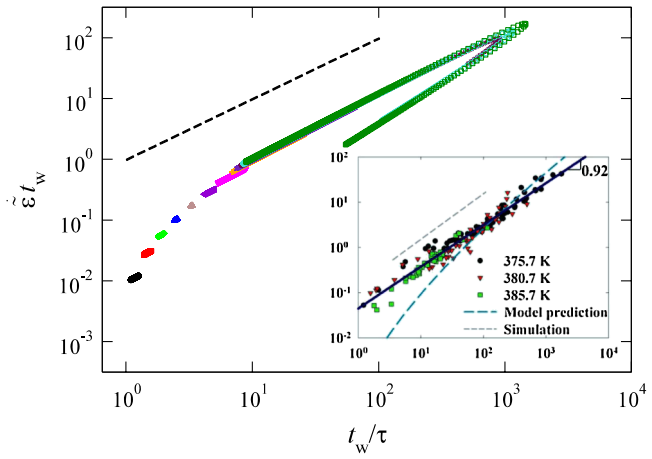

FIG. 3 (color online). For the same runs as in Fig. 2, during loading phase only, log-log plot of reduced strain rate against reduced relaxation rate. Inset: experimental data collapse with this plot, slope 0.92 (from [3]; reprinted by permission of AAAS). Partial collapse occurs here (dashed line is slope 1): while reentrant regions do not fully superpose, the slopes of the rising and decreasing curves remain comparable.

These successes are very encouraging. However, the model as formulated so far breaks down badly when the sample is unloaded. Here the experiments show a modest drop in τ immediately on removing the load, followed by a gradual recovery towards the predeformation value. The dotted line in Fig. 1 shows the prediction based on Eqs. (1)–(4); τ drops, but then falls much further before recovering. The reason for this behavior within our model is clear. In the strain-hardened regime, according to Eq. (1), the polymers carry a large (and largely elastic) tensile stress, which exceeds Σ_Y^s. Upon unloading, this acts backwards on the vitrified solvent, causing it to yield. The resulting $\tau(t)$ resembles a rerun of the initial loading experiment. Another discrepancy is that the value of $G^p \simeq 6$ MPa needed to fit the loading data is approximately 10 times larger than the rubbery modulus of the same material above its glass transition (see, e.g., [33]). This confirms that the strain-hardened modulus of polymer glasses does not primarily stem from single-chain entropic elasticity [24,28].

We now identify a physical mechanism that could account for both discrepancies. We invoke the well established phenomenon of large but viscous stresses that arise when chains are strained rapidly relative to their own relaxation time ($\dot{\varepsilon}\tau^p \gg 1$). Under such conditions, relatively small sections of polymer quickly approach full extension locally, forming a nearly one-dimensional multiply folded ("kinked") filament [34,35]. Further stretching occurs by migration and annihilation of neighboring kinks of opposite sign. During this process, a large fraction of the stress carried by the polymers is not entropic-elastic, but instead caused by viscous drag against extended subsections of chain. Upon unloading, a large fraction of this inelastic polymer stress disappears on a very rapid time scale [34]. This mechanism is closely related to "chain conformation hysteresis" of stretched chains, which causes a sudden loss of polymer stress on unloading with only modest relaxation of polymer conformations [36]. It implies violations of the linear relation between polymer stress and conformation assumed so far.

A full treatment [31,37–41] of this rather complex effect would entail replacing Eq. (1) with a more complex polymer model such as the multimode description developed in [34]. Rather than attempt this, we leave (1)–(4) intact but suppose phenomenologically that the effective polymer modulus drops by a certain factor, $G^p \rightarrow \theta G^p$, during unloading of the sample. The solid line in Fig. 1 shows the result for $\theta = 0.1$. This choice of θ is consistent with the fitted G^p being 10 times larger than the value expected from entropic elasticity alone. The polymer stress acting backwards on the solvent is now safely below the solvent yield stress; the result is a modest drop and then a slow increase in $\tau(t)$, as seen experimentally.

Overall, the success of our simplified model suggests that the striking time dependence of the segmental mobility under elongation, reported in [3], should be a robustly universal feature of near-T_g polymer glasses. However, the quantitative details strongly depend on dimensionless parameters such as G^s/G^p, μ, and θ. We cannot link these directly to microscopic physics, but such parameters can influenced by increasing polymer stiffness, adding small molecules, or introducing short side chains. (All of these should increase G^s/G^p, by raising the ratio of solventlike to polymeric degrees of freedom.) Our model may thus suggest design strategies for manipulating the evolution of $\tau(t)$, tailoring the mechanical responses of polymer glasses to suit particular design needs.

In conclusion, we have presented a simple model for polymer glasses that builds on concepts of rheological aging and rejuvenation in simple glassy fluids. Without attempting to capture every feature of the experiments of [3] (for instance, we do not address the nonexponential form of local relaxations), the minimal combination of a simple-aging fluid with a strain-dependent polymer stress can explain much of what happens when a polymer glass is subjected to elongational load. The unloading behavior is less easily explained, but consistent with a plausible modification of the same model, which crudely allows for the presence of nonelastic polymer stresses when $\dot{\varepsilon}\tau^p$ is large [34]. Although we do not address thermal or memory effects in this Letter, our model (with $\alpha = 0$) does predict that on heating to the stress-free liquid phase a lightly crosslinked sample that was plastically deformed as a glass will exactly recover its original shape [3].

Our work suggests that an accurate representation of aging and rejuvenation physics will form a key part of any more comprehensive theory of polymer glass rheology. It encourages the view that a more comprehensive account

of polymer glasses might be achieved by judiciously combining existing types of nonlinear rheological theory (describing nonglassy polymers and simple glasses, respectively). Quantitative progress along these lines might enable rapid advances towards the design of superior polymer glass materials.

M. E. C. is funded by the Royal Society. This work was funded in part by EPSRC EP/E030173. R. G. L. is partially supported from NSF under Grant No. DMR 0906587.

[1] T. C. B. McLeish, Adv. Phys. **51**, 1379 (2002).
[2] R. G. Larson, *Constitutive Equations for Polymer Melts and Solutions* (Butterworth-Heinemann, Boston, 1988).
[3] H.-N. Lee, K. Paeng, S. F. Swallen, and M. D. Ediger, Science **323**, 231 (2009).
[4] L. C. E. Struik, *Physical Aging in Amorphous Polymers and Other Materials* (Elsevier, New York, 1978).
[5] P. G. Debenedetti and F. H. Stillinger, Nature (London) **410**, 259 (2001).
[6] D. C. Hofmann *et al.*, Nature (London) **451**, 1085 (2008).
[7] P. Schall, D. A. Weitz, and F. Spaepen, Science **318**, 1895 (2007).
[8] J. M. Brader, M. E. Cates, and M. Fuchs, Phys. Rev. Lett. **101**, 138301 (2008).
[9] J. M. Brader, T. Voigtmann, M. Fuchs, R. Larson, and M. E. Cates, Proc. Natl. Acad. Sci. U.S.A. **106**, 15 186 (2009).
[10] S. M. Fielding, P. Sollich, and M. E. Cates, J. Rheol. **44**, 323 (2000).
[11] K. Chen and K. S. Schweizer, Europhys. Lett. **79**, 26 006 (2007).
[12] M. L. Falk and J. S. Langer, Annu. Rev. Condens. Matter Phys. **2**, 353 (2011).
[13] C. Derec, A. Ajdari, F. Lequeux, Eur. Phys. J. E **4**, 355 (2001).
[14] P. Coussot, Q. D. Nguyen, H. T. Huynh, and D. Bonn, Phys. Rev. Lett. **88**, 175501 (2002).
[15] B. Rinn, P. Maass, and J.-P. Bouchaud, Phys. Rev. Lett. **84**, 5403 (2000).
[16] H.-N. Lee and M. D. Ediger, Macromolecules **43**, 5863 (2010).
[17] R. A. Riggleman, H. N. Lee, M. D. Ediger, and J. J. de Pablo, Phys. Rev. Lett. **99**, 215501 (2007).
[18] H. N. Lee, R. A. Riggleman, J. J. de Pablo, and M. D. Ediger, Macromolecules **42**, 4328 (2009).
[19] M. Warren and J. Rottler, Phys. Rev. E **76**, 031802 (2007).
[20] M. Warren and J. Rottler, Phys. Rev. Lett. **104**, 205501 (2010).
[21] H. Eyring, J. Chem. Phys. **4**, 283 (1936).
[22] K. Chen and K. S. Schweizer, Phys. Rev. Lett. **102**, 038301 (2009).
[23] K. Chen and K. S. Schweizer, Phys. Rev. E **82**, 041804 (2010).
[24] K. Chen, E. J. Saltzman, and K. S. Schweizer, J. Phys. Condens. Matter **21**, 503101 (2009).
[25] R. N. Haward and G. Thackray, Proc. R. Soc. A **302**, 453 (1968).
[26] E. T. J. Klompen, T. A. P. Engels, L. E.Govaert, and H. E. H. Meijer, Macromolecules **38**, 6997 (2005).
[27] R. S. Hoy and C. S. O'Hern, Phys. Rev. E **82**, 041803 (2010).
[28] R. S. Hoy and M. O. Robbins, Phys. Rev. Lett. **99**, 117801 (2007).
[29] K. Nayak *et al.*, J. Polym. Sci., Part B: Polym. Phys. **49**, 920 (2011).
[30] P. J. Hine, A. Duckett, and D. J. Read, Macromolecules **40**, 2782 (2007).
[31] See Supplemental Material at http://link.aps.org/supplemental/10.1103/PhysRevLett.108.048301 for the lubrication theory, numerical methods, parameter estimations, and some additional results.
[32] L. C. A. van Breemen, E. T. J. Klompen, L. E. Govaert, and H. E. H. Meijer, J. Mech. Phys. Solids **59**, 2191 (2011).
[33] R. N. Haward, Macromolecules **26**, 5860 (1993).
[34] R. G. Larson, Rheol. Acta **29**, 371 (1990).
[35] E. J. Hinch, J. Non-Newtonian Fluid Mech. **54**, 209 (1994).
[36] J. P. Rothstein and G. H. McKinley, J. Non-Newtonian Fluid Mech. **108**, 275 (2002).
[37] M. M. Denn, Annu. Rev. Fluid Mech. **12**, 365 (1980).
[38] M. A. Matovich and J. R. A. Pearson, Ind. Eng. Chem. Fundam. **8**, 512 (1969).
[39] D. O. Olagunju, J. Non-Newtonian Fluid Mech. **87**, 27 (1999).
[40] W. H. Press *et al.*, *Numerical Recipes in C* (Cambridge University Press, Cambridge, 1988).
[41] *Physical Properties of Polymers Handbook*, edited by J. E. Mark (Springer, New York, 2007), 2nd ed.